Infrared SST Autonomous Radiometer (ISAR) Skin Temperature Observation and Skin-Bulk Temperature Differences in the Seas around Korean Peninsula, the Indian Ocean, and the Northwest Pacific

Kyung-Ae Park[1] , Hee-Young Kim[2], and Hye-Jin Woo[2]

[1] Department of Earth Science Education, Seoul National University, Seoul, Korea

[2] Department of Science Education, Seoul National University, Seoul, Korea

Abstract

- This study provides the recent ISAR observations in the seas surrounding the Korean Peninsula, the Indian Ocean, and the Northwest Pacific Ocean. To understand the characteristics of the sea surface temperature (SST) and its overall vertical structure, we collocated the ISAR temperatures and those from satellite SST, surface drifter, ARGO float, and shipborne thermosalinograph of R/V ISABU.
- The skin temperature was mostly lower than that of the satellite, and the difference between the two temperatures indicated a diurnal variation. Similar to the results of previous studies, the skin-bulk temperature differences tended to be amplified in the low wind speed. The amplitude of the diurnal fluctuation was inversely proportional to the wind speed, so it was more positively amplified during the day and a relatively small negative bias at night.
- The differences between surface drifter temperatures and ARGO temperatures also exhibited a diurnal variation with a negative bias in the night (before 9 AM), reaching its highest peak in the day (around 3 PM), and gradually decreased at night. The amplitudes of these temperature differences showed a seasonality with bimodality of the first peak in March-April and the secondary one in September-October.
- Under low wind condition, the drifter-ARGO temperature differences also showed dominant skin-bulk temperatures differences. The analyses of the temperature differences enabled to understand the comprehensive characteristics of vertical temperature structure and roles of wind speed and stability on diurnal/seasonal variations. More ISAR observations are needed for a substantial understanding of ocean warming in response to climate change.

ISAR Mounting

▲ **Figure.** Schematics of designs of the shipboard mounting system for a folding style and a sliding style fitted to the conditions of each vessel, and the features of ISAR mounted on guardrail of the ship for measurement tests on R/V ISABU.

R/V Cruises

	Test Cruise	Cruise 0	Cruise 1	Cruise 2	Cruise 3
Region	Eastern Coast of Korea	East China Sea South China Sea Indian Ocean	East Sea (Japan Sea)	Northwest Pacific	Northwest Pacific
R/V	Tamsa-2	ISABU	ISABU	ISABU	ISABU
Date	21 Feb 2019	27 March 2019 – 14 April 2019	23 April 2020 – 4 May 2020	13 May 2020 – 26 May 2020	31 July 2020 – 29 August 2020
Duration	1 day	18 days	13 days	19 days	30 days
Temperature Range	8-12°C	25-34°C	9-22°C	14-31°C	20-35°C

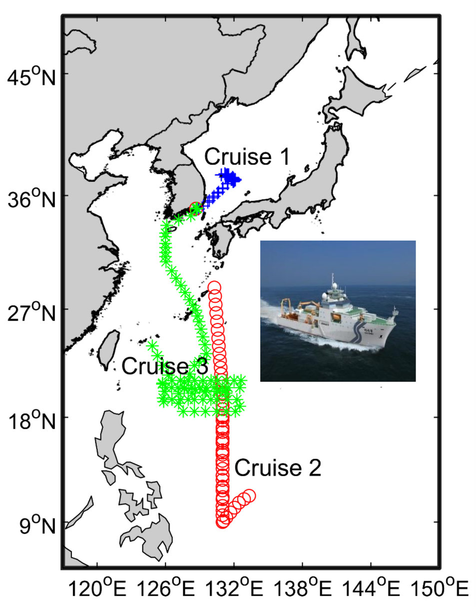

	ISABU
Gross Tonnage	5,994 tons
Full Length	99.8 m
Width	18.0 m
Maximum Speed	15 knots, 12 knots (cruise)
Sensors	AWS
	DGPS
	Thermosalinograph Accuracy: 0.003°C , Resolution: 0.0002°C
	CTD (Accuracy : 0.001°C)
	http://kiost.ac.kr/eng/sub02_05_01.do

▲ **Table.** Information of cruises in the seas around Korea, the East China Sea, the South China Sea, the Indian Ocean, and the northwest Pacific

▲ **Table** Information of R/V ISABU

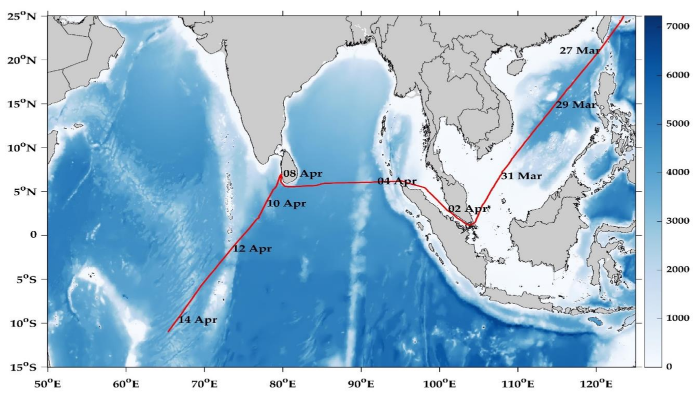

▲ **Figure** Tracks of three cruises in the East Sea and NW Pacific.

▲ **Figure** Cruise track from Busan to the Indian Ocean from 21 March to 14 April 2019

Retrieval of ISAR Skin Temperature

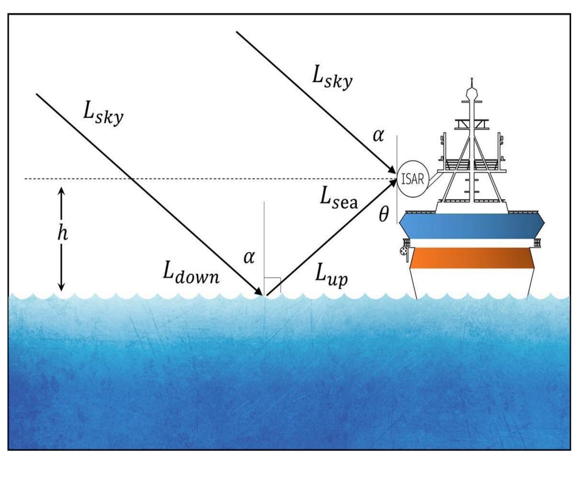

$$L_{sea}(\lambda) = \varepsilon(\lambda,\theta)B(SST_{skin},\lambda) + [1-\varepsilon(\lambda,\theta)]L_{sky}.$$

Output signal of radiometer (sea)

$$S_{sea} = \int_{\lambda_1}^{\lambda_2} \zeta(\lambda)\{\varepsilon(\lambda,\theta)B(SST_{skin},\lambda) + [1-\varepsilon(\lambda,\theta)]L_{sky}(\lambda)\}\,d\lambda,$$

Output signal of radiometer (sky)

$$S_{sky} = \int_{\lambda_1}^{\lambda_2} \zeta(\lambda)L_{sky}(\lambda)\,d\lambda.$$

Within the narrow wave band 9.5-11.5 μm, $\varepsilon(\lambda,\theta)$ and $B(\lambda,T)$ vary only slowly with wavelength

→ Can be given as band-averaged value

$$S_{sea} = \zeta_B\{\varepsilon_B(\theta)B_B(SST_{skin}) + [1-\varepsilon_B(\theta)]L_{B,sky}\},$$

$$S_{sky} = \zeta_B L_{B,sky},$$

$$\zeta_B B_B(SST_{skin}) = \frac{S_{sea} - [1-\varepsilon_B(\theta)]S_{sky}}{\varepsilon_B(\theta)}.$$

▲ **Figure.** A schematic diagram of radiation rays penetrated into the ISAR installed on a ship, where h is a height of the ISAR from the sea surface, L_{sky} is the sky incident radiation, L_{down} is the downwelling radiance incident on the sea surface, L_{up} is the upwelling radiance from the sea surface, and L_{sea} is the radiance originating from the sea surface, θ is an angle between the nadir of the ISAR and the ray of Lsea into the ISAR.

U_{10} Conversion

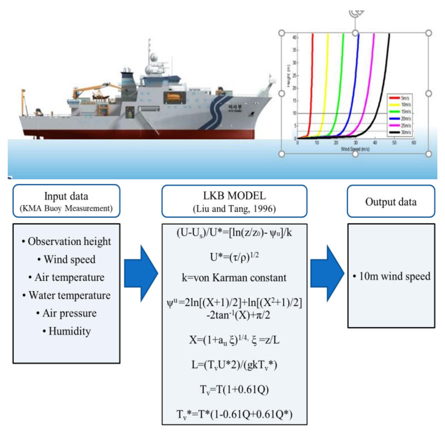

▲ **Figure.** Conversion procedure of AWS wind measurements, at a height of 36 m of R/V ISABU, to U_{10} by using LKB model.

ISAR Observations for Skin SST

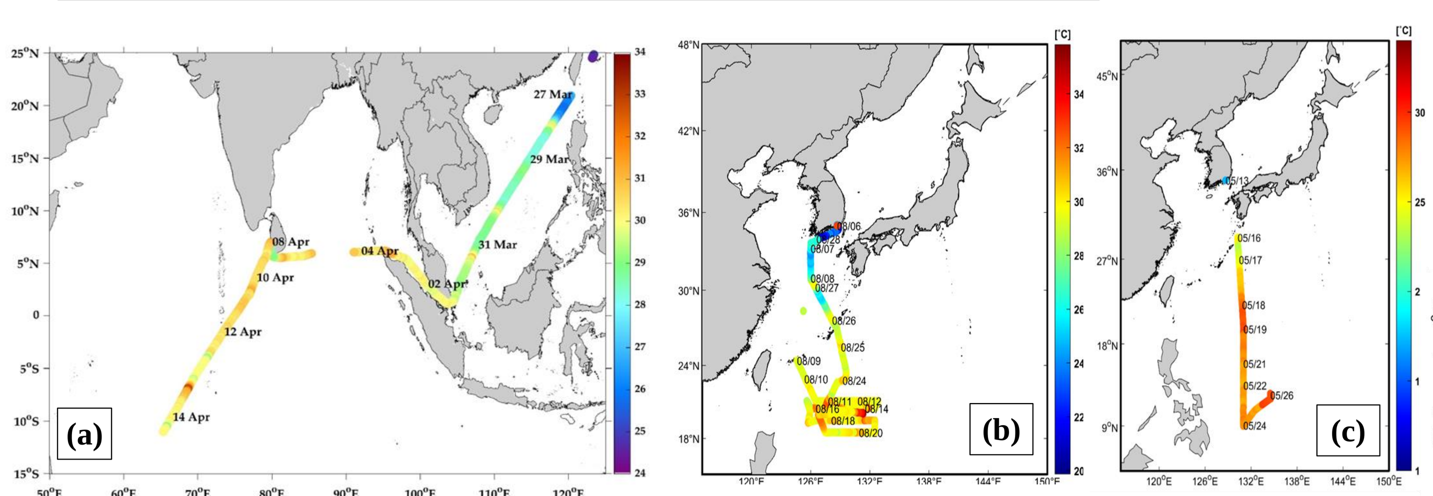

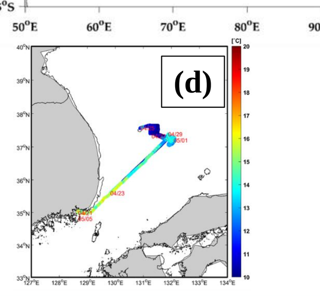

▲ **Figure** ISAR-observed skin SST (SSST) (a) along the cruise track from March 27 to 14 April in the Indian Ocean, (b) along the cruise line from Busan, Korea to the East China Sea and the northwest Pacific, (c) along another cruise track from Busan to the south in the northwest Pacific, and (c) from Busan to the offshore region of the East Sea. The rainbow colors represent the retrieved SSST from ISAR observed data.

Comparisons of ISAR Temperature

AMSR2 SST

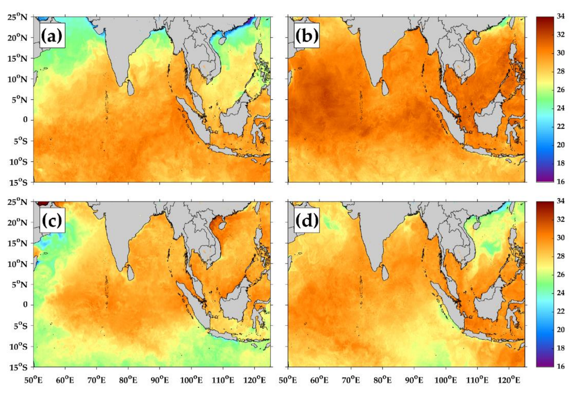

▲ **Figure.** Seasonal variation of AMSR-2 sea surface temperature in (a) February, (b) March, (c) August, and (d) November 2019.

AMSR2 SST

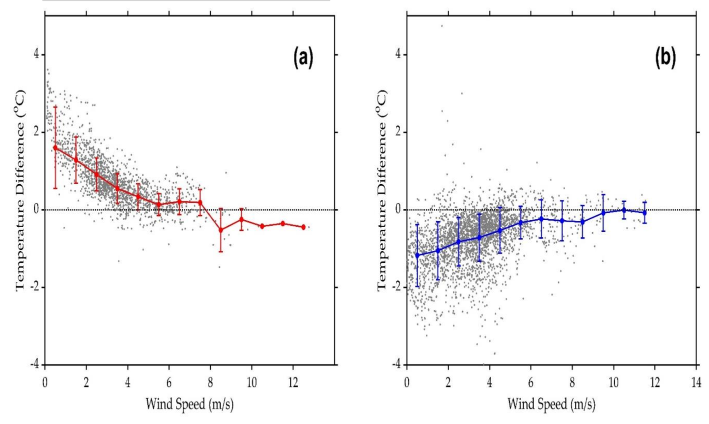

▲ **Figure.** Along-track temperature difference between (a) daytime and (b) nighttime **AMSR2** SST as a function of wind speed. This shows contrast of SST differences: overestimation during a day and underestimation during a night at low-wind speeds.

ISAR - AMSR2

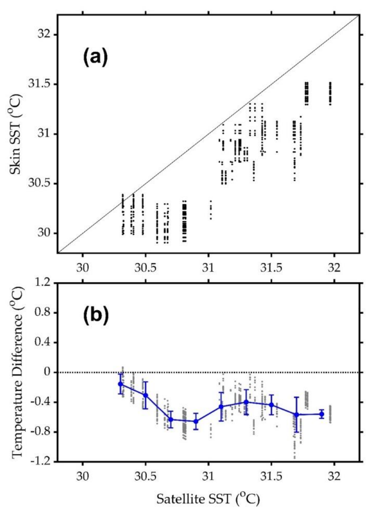

▲ **Figure.** Comparison of ISAR skin SST and **AMSR2** SST in the Indian Ocean (2012-2019)

Drifter - ARGO

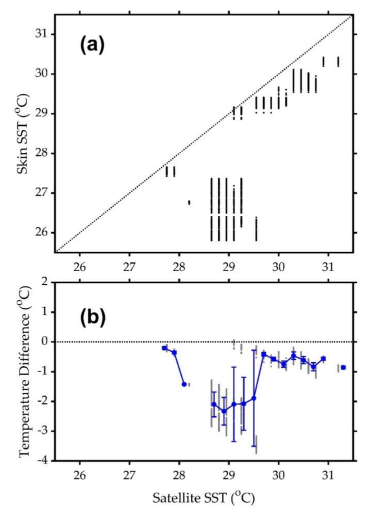

▲ **Figure.** Comparison of drifter SST and **ARGO** surface temperature in the Indian Ocean (2012-2019)

Temporal Variation of Temperature Differences

Drifter – ARGO (Seasonal Variations)

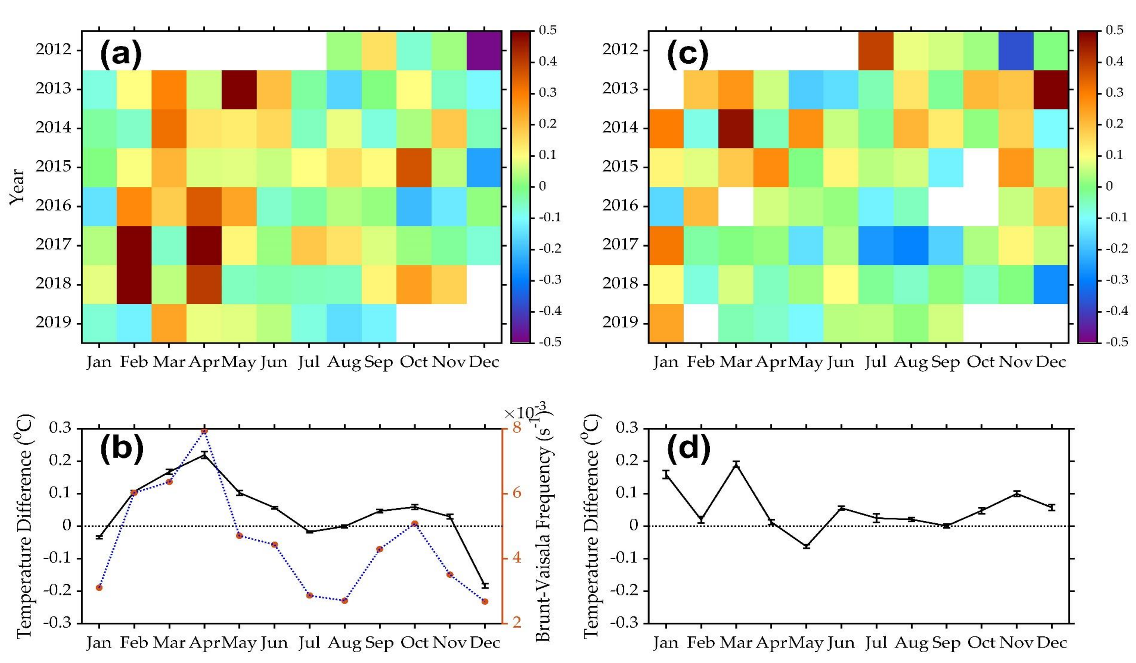

▲ **Figure.** Yearly and monthly distribution of differences between surface drifter sea surface temperature data (SST) and ARGO float water temperature for the (a) Northern Hemisphere and (b) the Southern Hemisphere. The red dots and dotted line represent Brunt-Vaisala frequency (s^{-1}) of water comumn of upper ocean

Drifter – ARGO (Diurnal Variations)

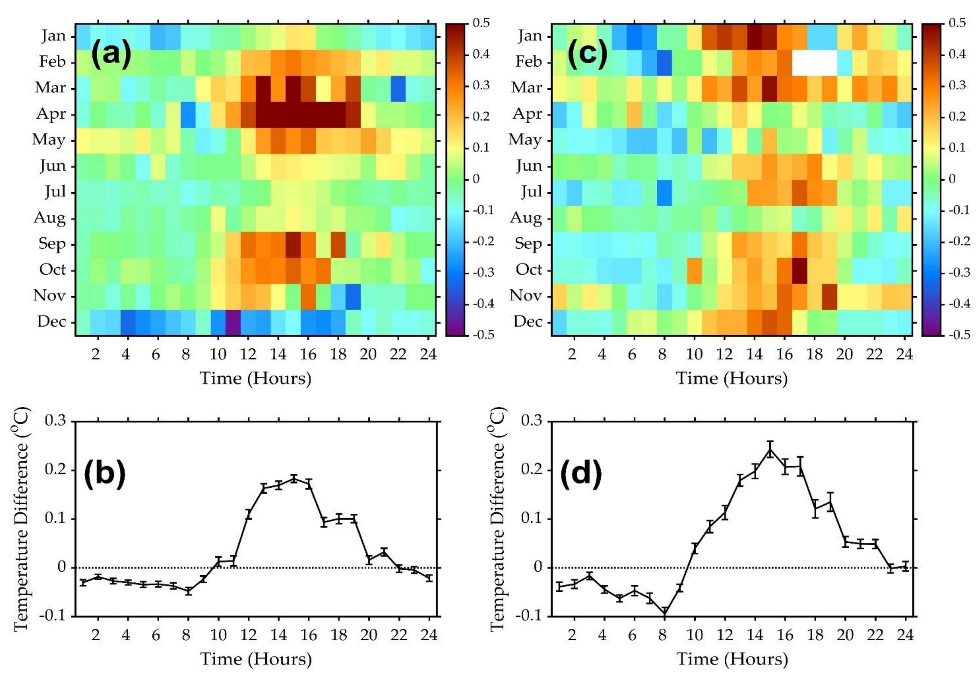

▲ **Figure.** Monthly and hourly distribution of differences between surface drifter sea surface temperature data (SST) and ARGO float water temperature for the (a) Northern Hemisphere and (b) the Southern Hemisphere in the Indian Ocean.

Effect of Wind Speed on Diurnal Variations

Drifter – ARGO

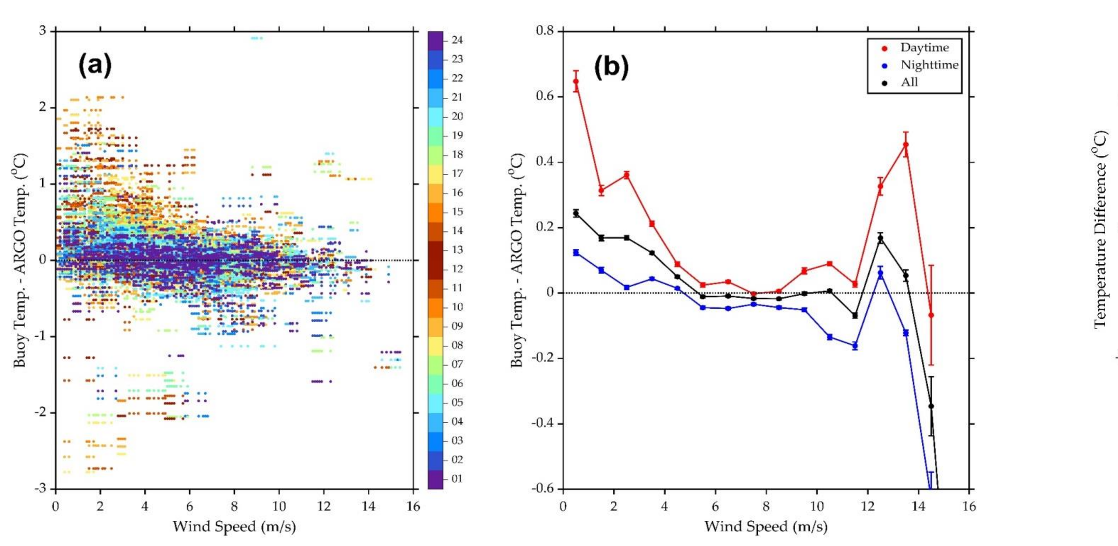

▲ **Figure.** Distributions of the SST differences (Buoy SST – Argo SST) as a function of the wind speed (ms^{-1}), where the bars represent the mean standard deviations of SST differences for each interval.

Drifter – ARGO

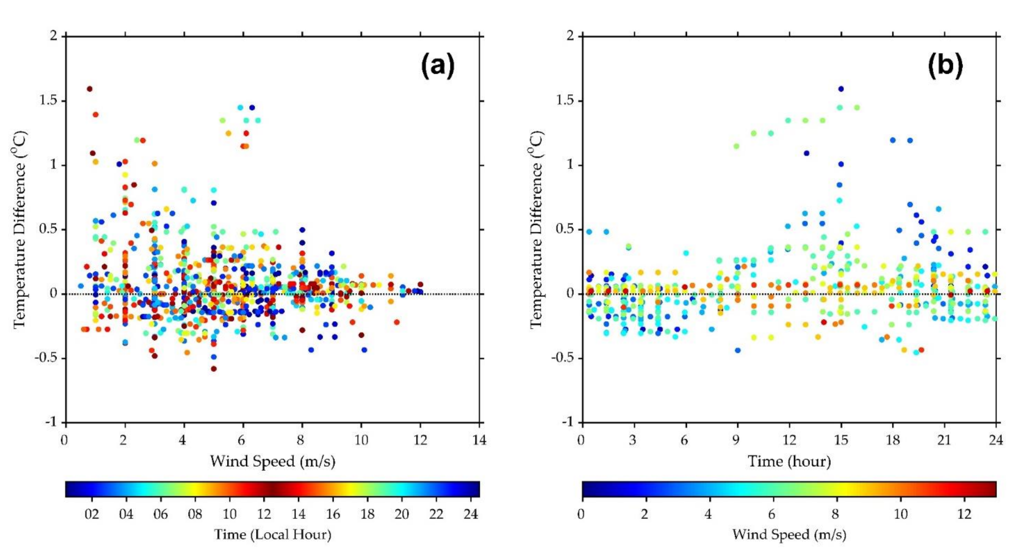

▲ **Figure.** Distributions of the SST differences (Buoy SST – Argo SST) as a function of (a) the wind speed (ms^{-1}) where colors represent time in local hours and (b) hour where the colors represent the wind speed of each dot.

Relation to Stratification

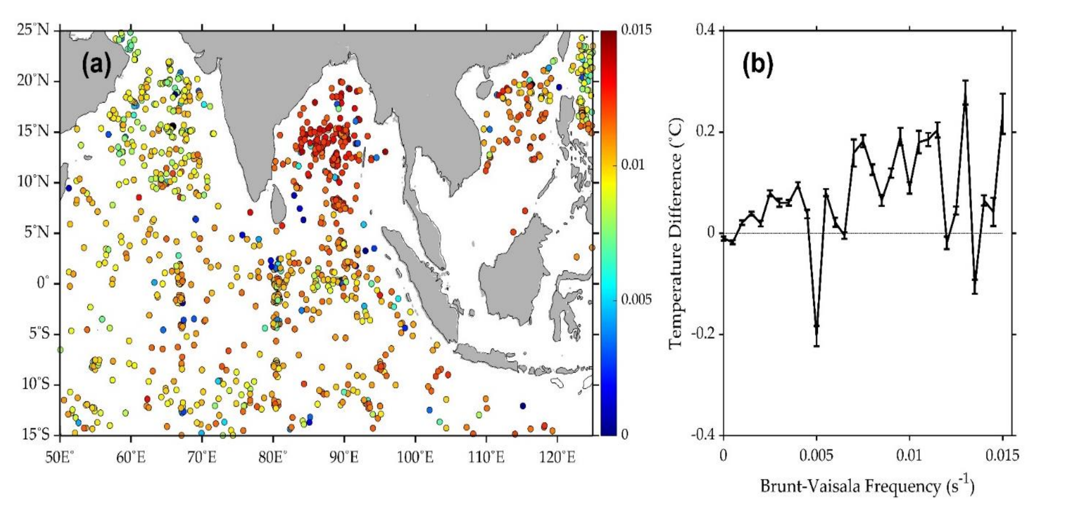

▲ **Figure.** Distribution of (a) Brunt-Väisälä Frequency in the Indian Ocean and (b) SST difference between drifter SST and ARGO temperature according to Brunt-Väisälä Frequency

Schematic

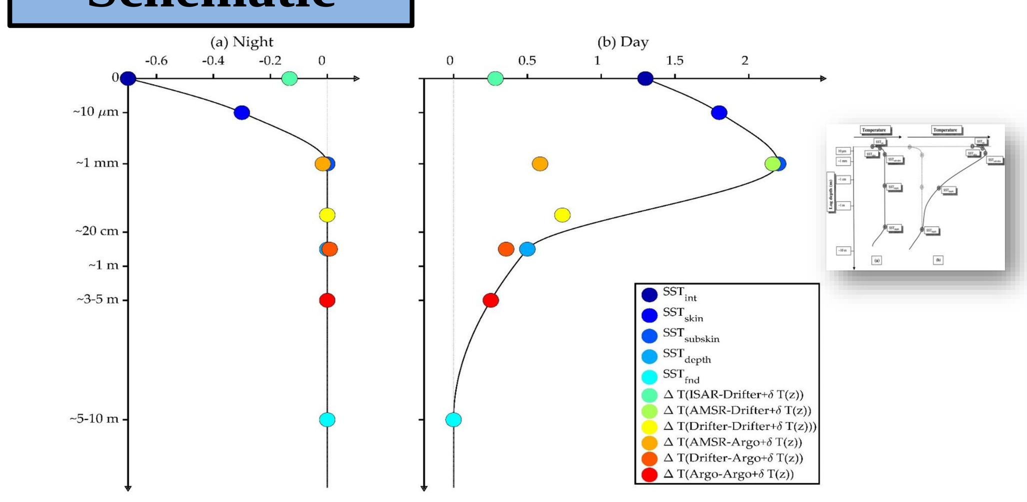

▲ **Figure.** Schematic of vertical distributions of SST differences during (a) the night and (b) the day based on the comparisons of temperature differences among ISAR skin temperatures, AMSR2 satellite SSTs, drifter temperatures, and ARGO temperatures, which is similar to Donlon et al.(2002).

Multi-Comparisons

	Datasets	Global (°C)	NW Pacific Ocean (°C)	Seas around Korea (°C)
RMSE	Drifter - ARGO SST	0.57	0.52	0.75
	AMSR2 - Drifter SST	0.64	0.61	0.78
BIAS	Drifter - ARGO SST	-0.06	-0.008	-0.01
	AMSR2 - Drifter SST	0.07	0.04	0.01

▲ **Table.** RMSE and bias errors between multi SST datasets (drifter SST, ARGO SST, AMSR2 SST) in the global ocean, northwest Pacific, the seas adjacent to Korean peninsula for the period from 2012 to 2019.

	Datasets	Northwest Pacific (°C)	East Sea (°C)
RMSE	ISAR – TSG	0.61	0.76
BIAS	ISAR - TSG	-0.13	-0.70

▲ **Table.** RMSE and bias errors between ISAR skin temperature and thermosalinograph (TSG) temperatures in the northwest Pacific and the seas adjacent to the Korean peninsula (the East Sea) for the period from 2019 to 2020.

Conclusion

- The study presents the comparisons of ISAR skin temperature measurements with other SST meansurements (TSG, AMSR2 satellite SST, surface drifters, ARGO float) in the seas around Korean Peninsula, the East China Sea, the Indian Ocean, the Northwest Pacific.
- The observed skin-bulk temperature differences well express wind-induced effects and diurnal changes as mentioned in well-known previous studies. The effect of the wind speed showed a diurnal variations by addressing the importance of the effect of wind speed for understanding the skin-bulk temperature differences and air-sea interactions. As the stability of the water layer increased, the vertical temperature difference also increased.
- A schematic of temperature differences between multi temperatures (ISAR skin SST, satellite SST, drifter temperature, thermosalinograph temperature, ARGO temperature) represent daytime and nighttime vertical profiles similar to Donlon et al.(2002)

[Acknowledgement] This study was supported by the National Research Foundation of Korea (NRF), grant funded by the Korean government (MSIT) (No. 2020R1A2C2009464).